J. Electrochem. Sci. Eng. **12(5)** (2022) 819-828; http://dx.doi.org/10.5599/jese.1278

Open Access : : ISSN 1847-9286

https://pub.iapchem.org/ojs/index.php/JESE

Original scientific paper

Mechanical and microstructural properties of yttria-stabilized zirconia reinforced Cr3C2-25NiCr thermal spray coatings on steel alloy

Sukhjinder Singh[1,✉], Khushdeep Goyal[1] and Rakesh Bhatia[2]

[1]*Department of Mechanical Engineering, Punjabi University, Patiala, India*

[2]*Yadavindra Department of Engineering, Punjabi University Guru Kashi Campus, Damdama Sahib, India*

Corresponding author: ✉*sukhjindermoga@gmail.com; Tel.: +91-9876785500*

Received: February 3, 2022; Accepted: March 21, 2022; Published: March 29, 2022

Abstract

In this research work, nano yttria-stabilized zirconia (YSZ) reinforced Cr3C2-25NiCr composite coatings were prepared and successfully deposited on ASME-SA213-T-22 (T22) boiler tube steel substrates using high-velocity oxy-fuel (HVOF) thermal spraying method. Different nanocomposite coatings were developed by reinforcing Cr3C2-25NiCr with 5 and 10 wt.% YSZ nanoparticles. The nanocomposite coatings were analysed by scanning electron microscope (SEM)/Energy-dispersive X-ray spectroscopy (EDS) and X-ray diffraction (XRD) technique. The porosity of YSZ- Cr3C2-25NiCr nanocomposite coatings was found to be decreasing with the increase in YSZ content, and hardness has been found to be increasing with an increase in the percentage of YSZ in the composite coatings. The coating of 10 wt.% YSZ-Cr3C2-25NiCr showed the lowest porosity, lowest surface roughness, and highest microhardness among all types of coatings. This may be due to the flow of YSZ nanoparticles into the pores and gaps that exist in the base coatings, thus providing a better shield to the substrate material.

Keywords

Boiler steel tube; composite nanoparticles; coatings; surface roughness; porosity; hardness

Introduction

Traditional steels used in thermal power plants are susceptible to corrosion [1,2]. In the recent past, researchers have applied several types of coatings to improve the erosion and corrosion resistance of these steels [3-5]. Thermal spray coating techniques are a key tool for developing coatings that improve component performance and longevity [6,7]. In recent years, these coatings have become more important. Coatings with high anti-corrosion qualities have been developed as a result of advancements in powder manufacture and innovations in thermal spraying techniques [8-10]. In terms of substrate material chemical composition, these procedures have no special material limitations [11]. On boiler tube steel components, flame spraying, plasma spraying, arc spraying,

and high-velocity oxygen fuel (HVOF) methods can generate coatings of a few millimeters thickness with a high microhardness value [12-15]. Because of its cost-effectiveness and versatility, the HVOF method has been classified as an adaptable technique [16-18]. The qualities of the substrate material are unaffected by the HVOF coating procedure [19].

In the recent past, various researchers have used thermal spraying techniques to develop various types of coatings on boiler steels to increase their properties. The coatings produced by the thermal spraying method are porous in nature and have many local micro-cracks or through pores [20-22]. Corrosive fluids and chemicals attack the substrate steels through these pores and micro-cracks. Therefore, there is still scope for improvement in the mechanical and microstructural properties of these coatings [23-25]. Many researchers have compared conventional coatings to nanostructured coatings, and many improvements in mechanical and microstructural properties of as-sprayed materials were observed, including an increase in microhardness, a decrease in porosity, a decrease in surface roughness, and a decrease in erosion rate, among other things [26-29]. Many authors have reported the development of Cr3C2-25NiCr coatings on steel alloys, but literature related to nano yttria-stabilized zirconia (Y_2O_3/ZrO_2) (YSZ) reinforced composite coatings is not available. Therefore, there is scope to develop new nano yttria-stabilized zirconia (YSZ) mixed Cr3C2-25NiCr nanocomposite coatings and subsequently deposit and investigate the microstructure, porosity, and microhardness of these newly developed composite coatings on boiler tube steel.

In this research work, HVOF sprayed 5 and 10 weight percent YSZ-Cr3C2-25NiCr nano-coatings were developed and deposited on T22 boiler tube steel. The microstructure, porosity and micro-hardness of these newly developed composite coatings have been investigated. HVOF thermal spraying technique was used in this research work because the coatings produced with the HVOF method have high adhesive strength with the base material and also individual splats have high cohesive strength [30-31]. Ksiazek *et al*. [20] observed that this spraying process provides homogeneous coatings having a low value of porosity along with high hardness.

Experimental

Substrate material

The measured and nominal compositions of T22 steel are shown in Table 1. The samples with dimensions of 22×15×5 mm were manufactured from the boiler tube. Silicon carbide paper was used to polish the cut samples. Before applying different coatings, the samples were shot blasted with alumina powder of grit 45.

Table1 *Chemical composition of T-22 steel*

	Content, wt.%									
	C	Mn	Si	S	P	Cr	Mo	V	Ni	Fe
Nominal	0.15	0.3-0.6	0.5-1	0.03	0.03	1.9-2.6	0.07-1.13	--	--	Bal.
Actual	0.148	0.524	0.762	0.039	0.0129	2.692	0.928	0.031	0.019	Bal.

Coating powders

Commercially available blend Cr3C2-25NiCr powder was mixed with 5 and 10 wt.% YSZ using low energy ball milling to prepare different coating powders and the composition of different powders is shown in Table 2. To prepare Cr3C2-25NiCr mixed with 5 wt.% YSZ (Y_2O_3/ZrO_2) mixture, 950 g of Cr3C2-25NiCr was mixed with 50 grams of YSZ. Other compositions were prepared in a similar manner. The mixed powders were rolled for four hours ceaselessly at a speed of 200 rpm [32,33].

Table 2. *Composition of feed stock powders*

Feed stock powder	Base powder Cr3C2-25NiCr content, wt.%	Content of reinforced YSZ nano powder, wt.%
Cr3C2-25NiCr	100	0
5 wt.% YSZ- (Cr3C2-25NiCr)	95	5
10 wt.% YSZ- (Cr3C2-25NiCr)	90	10

Formulation of coating

The conventional Cr3C2-25NiCr, 5 and 10 wt.% YSZ reinforced Cr3C2-25NiCr nanocoatings were deposited on T22 boiler steel substrates with the HVOF process at Metallizing Equipment Company Limited, Jodhpur, India. The spraying process was carried out using a commercial HIPOJET-2100 device. Before deposition of the coatings, the samples were grit blasted with alumina powder. Coatings with a thickness of around 250 µm were deposited. The process parameters of the HVOF spraying method are shown in Table 3. During the spraying procedure, these process parameters were kept constant.

Table 3. *HVOF spraying process parameters*

Oxygen flow rate	280 L min^{-1}
Fuel (acetylene) flow rate	100 L min^{-1}
Air-flow rate	600 L min^{-1}
Spray distance	200 mm
Powder feed rate	25 g min^{-1}
Fuel pressure	1.6 kg cm^{-2}
Oxygen pressure	3.00 kg cm^{-2}
Air pressure	4.40 kg cm^{-2}

Characterization of nanocomposite coatings

The uncoated samples were cut into sections and mounted in epoxy. Before the metallurgical inspection, the mounted samples were polished. The coatings were examined using XRD, SEM/EDS, and cross-sectional elemental analysis. The microhardness of the cross-section of all coated samples was assessed using a Mitsubishi microhardness tester. On the coating–substrate interface, the microhardness was measured at specified intervals along the cross-section.

LEICA Image analyser software was used to evaluate the porosity of conventional Cr3C2-25NiCr, 5 and 10 wt.% YSZ reinforced Cr3C2-25NiCr nanocomposite coatings. Before evaluating porosity, the specimens were polished. The pore area size is calculated using a computer-based porosity analysis technique that converts grey-level areas (pore areas) into a background that is different from the rest of the microstructure. The porosity value is then calculated by counting the number of pixels of background colour. For each type of coated specimen, the average of five porosity measurements was calculated.

Results

Coating thickness measurement

The thickness of conventional Cr3C2-25NiCr, 5 and 10 wt.% YSZ reinforced Cr3C2-25NiCr nano-composite coatings was measured with the help of Minitest-2000 thin film thickness gauge (Make: ElektroPhysik Koln Company, Germany, precision ±1 µm) during the spraying process and are shown in Table 4. The thickness of the coatings was evaluated along the cross-section of the specimens and the thickness has been found in the desired range [34-36].

Porosity analysis

Thermal spray coatings are porous, and porosity has a significant impact on coating qualities. Less porous coatings provide superior corrosion protection, according to the literature. The apparent porosity measurements of Cr3C2-25NiCr, 5 and 10 wt.% YSZ reinforced Cr3C2-25NiCr nano-composite coated T22 steel specimens are shown in Table 4. For all samples, the porosity values of the HVOF-sprayed Cr3C2-25NiCr coating were less than 2 %. The numbers in Table 4 show that as the YSZ concentration in the nanocomposite coating increased, the porosity value also decreased. It is obvious that 10 wt.% YSZ-Cr3C2-25NiCr coating has the lowest porosity value. The surface roughness values for Cr3C2-25NiCr, 5 and 10 wt.% YSZ reinforced Cr3C2-25NiCr nanocomposite were found to be 3.75, 3.14 and 2.43 µm, respectively.

Table 4. *Average coating thickness and porosity values for different coatings*

Substrate	Coating type	Coating thickness, µm	Porosity, %	Average surface roughness, µm
ASME-SA213-T22	Cr3C2-25NiCr	251	1.81	3.75
	5 wt.% YSZ-(Cr3C2-25NiCr)	258	1.57	3.14
	10 wt.% YSZ-(Cr3C2-25NiCr)	252	1.25	2.43

Microhardness measurement

The microhardness profiles across the cross-section of Cr3C2-25NiCr, 5 and 10 wt.% YSZ reinforced Cr3C2-25NiCr nanocomposite coated specimens are shown in Figure 3. The micro-hardness values of T22 steel were in the range of 242-318 HV. The microhardness measurements for Cr3C2-25NiCr, 5 and 10 wt.% YSZ reinforced Cr3C2-25NiCr nanocomposite coated specimens were in the range of 918-978 1018-1093 and 1088-1168 HV, respectively. It is clearly seen in Figure 1 that with the increase of YSZ in the Cr3C2-25NiCr matrix, the micro-hardness value increased. The nano YSZ particles were able to increase the microhardness of HVOF sprayed Cr3C2-25NiCr coatings. The microhardness profiles clearly show that the hardness through the coating cross-section is nearly uniform for all coated specimens.

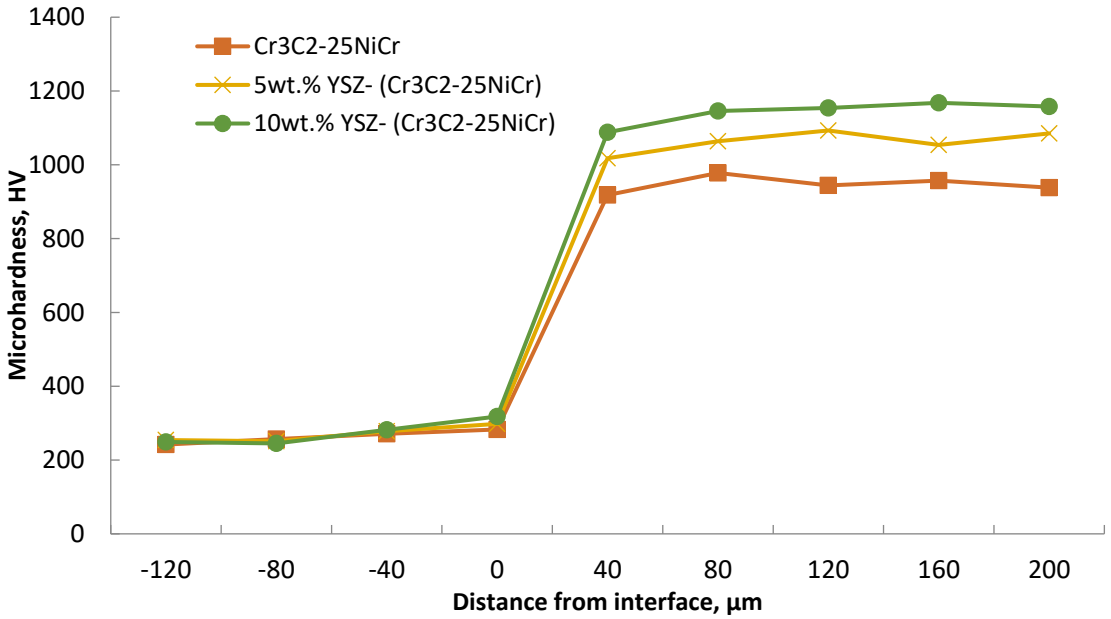

Figure 1*. Microhardness profiles of Cr3C2-25NiCr, 5 wt.% and 10 wt.% YSZ reinforced Cr3C2-25NiCr nanocomposite coatings across the cross-section*

X-ray diffraction analysis

The X-ray diffraction analysis for the surfaces of Cr3C2-25NiCr, 5 and 10 wt.% YSZ reinforced Cr3C2-25NiCr nanocomposite coated specimens was done, and the XRD patterns are shown in Figure 2(a-c). XRD profile of the HVOF sprayed Cr3C2-25NiCr coated T22 boiler tube steel sample showed chromium as the main phase, along with traces of Ni. The XRD profile of the Cr3C2-25NiCr coating reinforced with and 10 wt. % YSZ nanoparticles revealed that chromium and carbon are present as a major phase, and nickel, yttrium, and zirconium as minor phases. The increase in the formation of non-crystalline amorphous phases occurs because of very fast cooling during the spraying process. The presence of different phases and their proportion mostly depend on the process conditions at the time of the depositing of the coating powder on the base material.

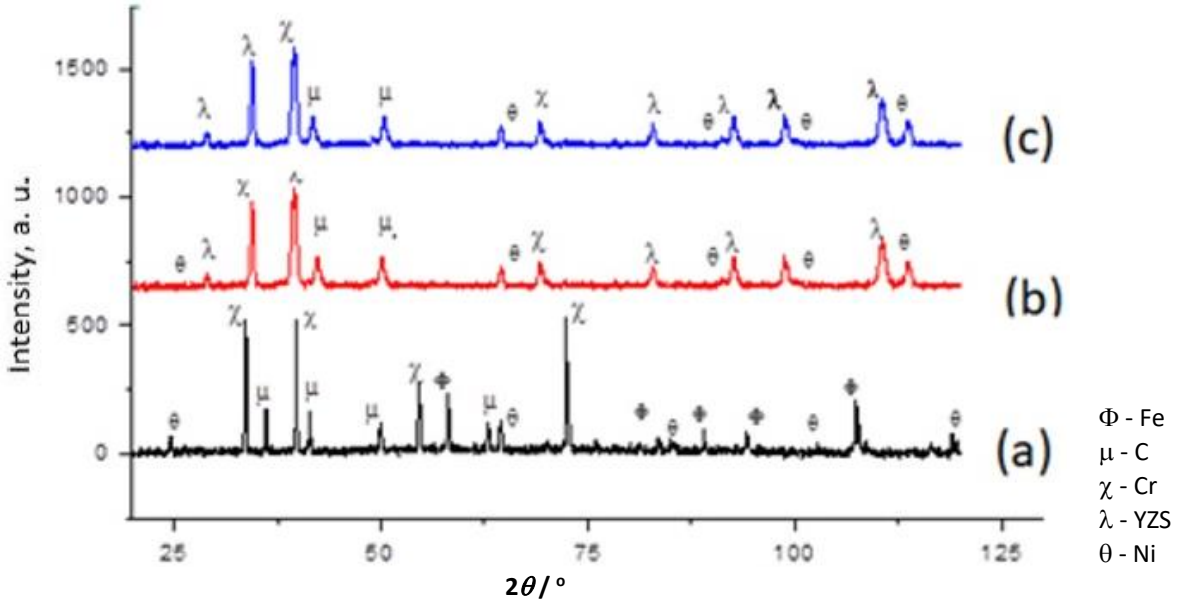

Figure 2. *XRD profile of: (a) Cr3C2-25NiCr; (b) 5 wt.% YSZ-(Cr3C2-25NiCr); (c) 10 wt.% YSZ-(Cr3C2-25NiCr)*

FE-SEM/Energy dispersive X-ray spectroscopy

FE-SEM micrographs with energy-dispersive X-ray spectroscopy analysis for HVOF sprayed Cr3C2-25NiCr, 5 and 10 wt.% YSZ reinforced Cr3C2-25NiCr nanocomposite coatings on T22 boiler steel are shown in Figure 3. The microstructure of Cr3C2-25NiCr coating is dense, consisting of inter-locked particles with regular shape, as shown in Figure 3(a). In the microstructure of the coating, several oxide stringers can also be visible. The YSZ nanoparticles have been uniformly diffused in the Cr3C2-25NiCr matrix, as shown in Figures 3(b) and 3(c). The dense and uniform layer of the coating was obtained by the reinforcement of nanoparticles of YSZ. The microstructures reveal that uniform coalescence of nano YSZ has occurred with base Cr3C2-25NiCr matrix in composite coating. As demonstrated in Figures 3(b) and 3(c), energy dispersive spectroscopy examination revealed the elemental composition of the various coatings that were found to be comparable to that of the feedstock powder. EDS analysis of Cr3C2-25NiCr coating revealed the presence of Fe and Si in the composition, which may be due to the diffusion of Fe and Si from the substrate to the coating matrix due to porosity in conventional coating.

The microstructure of the cross section of Cr3C2-25NiCr, and 10 wt.% YSZ reinforced Cr3C2-25NiCr nanocomposite coatings on T22 boiler steel is shown in Figure 4. The cross-sectional images indicate splat-like morphology of coatings, which might be due to the re-solidification of molten droplets.

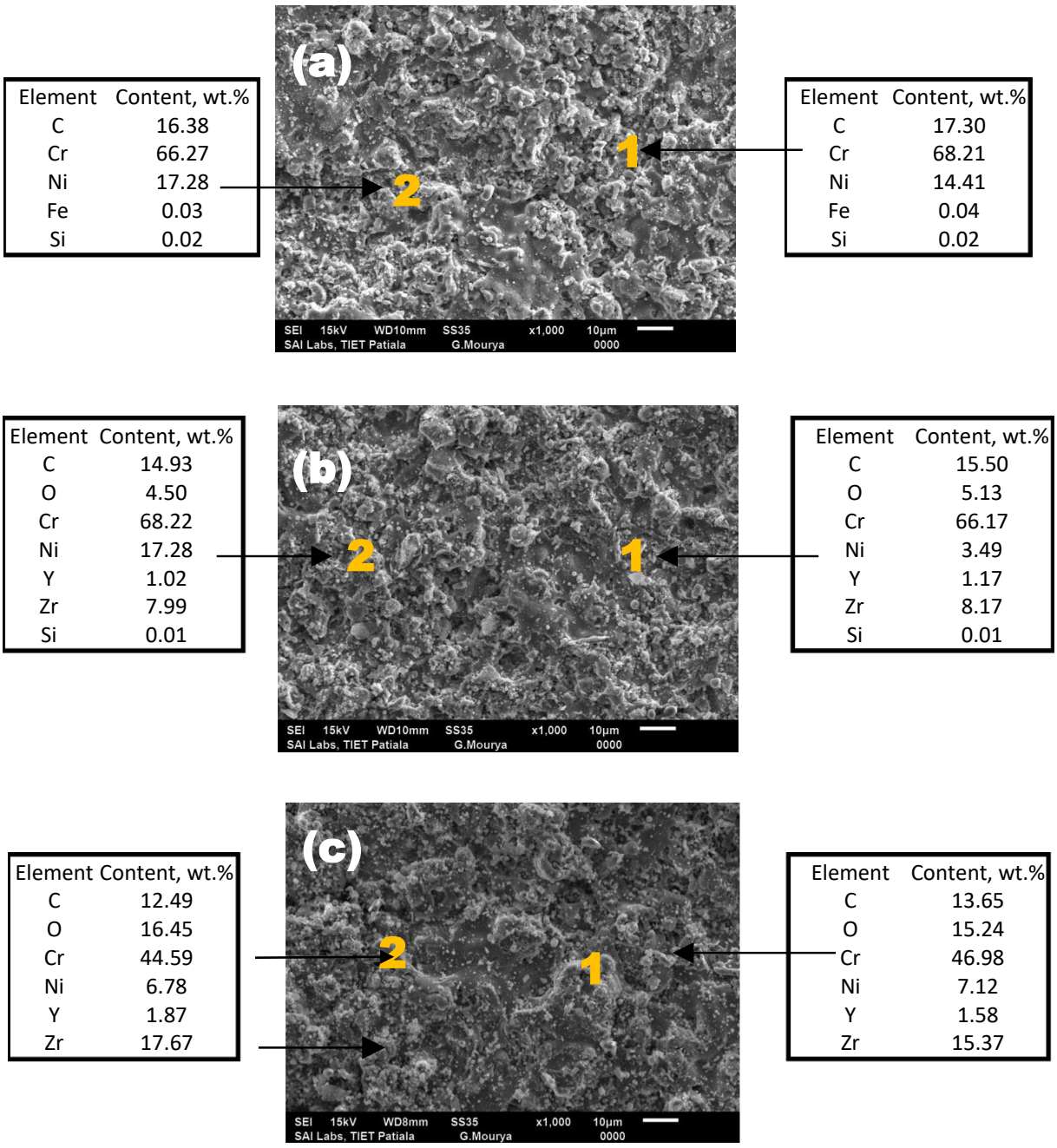

Figure 3. *FE-SEM with EDS analysis of HVOF sprayed coatings: (a) Cr3C2-25NiCr; (b) 5 wt.% YSZ- (Cr3C2-25NiCr); (c) 10 wt.% YSZ- (Cr3C2-25NiCr)*

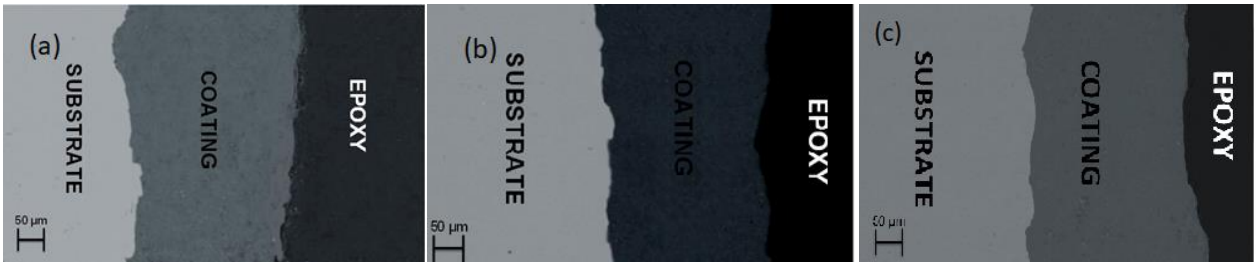

Figure 4. *Cross-sectional morphology of HVOF sprayed coatings: (a) Cr3C2-25NiCr; (b) 5 wt.% YSZ- (Cr3C2-25NiCr); (c) 10 wt.% YSZ- (Cr3C2-25NiCr)*

Discussion

The coating thickness of all coatings was measured along the cross-section of the coated specimens. The coating thickness was in the range of 251-258 µm, which was found to be in the desired

range as reported in the previous work for HVOF coatings [37]. The porosity of the conventional Cr3C2-25NiCr coating on T22 boiler tube steel was found to be 1.81%, which further decreases with the addition of nano YSZ to the Cr3C2-25NiCr coating matrix. The porosity values of 5 and 10 wt.% YSZ reinforced Cr3C2-25NiCr nanocomposite were observed as 1.57 and 1.25 %, respectively. The porosity of nanocomposite coatings decreased as the nanoparticles of nano YSZ filled the pores and interlocked the grains of the Cr3C2-25NiCr coating matrix. Improvement in surface roughness value was observed by the addition of the nanoparticles of YSZ in the Cr3C2-25NiCr coating powder. The surface roughness values for the Cr3C2-25NiCr, 5 and 10 wt.% YSZ reinforced Cr3C2-25NiCr nanocomposite coated samples were found to be 3.75 µm, 3.14 and 2.43 µm, respectively. Better surface characteristics were observed for 10 wt.% percent YSZ reinforced Cr3C2-25NiCr nanocomposite coating as compared to the conventional Cr3C2-25NiCr coating, as the surface roughness decreased because of the addition of YSZ nanoparticles. The decrease in porosity with the addition of carbon nanotubes has also been reported in the literature by Khesri *et al.* [38] and Guo *et al*. [39]. Goyal and Goyal [40] also reported that carbon nanotubes interlocked the particles of Cr3C2–20NiCr and improved the mechanical and microstructural properties of conventional Cr3C2–20NiCr coating.

In comparison to the base material, the microhardness values of all coated specimens were found to be extremely high, as shown in Figure 1. Microhardness values for typical Cr3C2–25NiCr ranged from 918 to 978 Hv. With an increase in nano YSZ weight percent in the Cr3C2–25NiCr matrix, microhardness values improved even further. The inclusion of nanoparticles in the coating matrix improved indentation resistance. The high heat conductivity of YSZ may result in increased melting and, as a result, an increased microhardness of YSZ reinforced coatings. The nano YSZ particles were uniformly scattered in Cr3C2–25NiCr matrix, filling the pores in the coating matrix, which resulted in a decrease in the porosity of the matrix. According to Tian *et al.* [41], the increase in hardness can be attributed to a decrease in porosity of the coating matrix and may also be due to dispersion hardening.

Cr and Ni are the main phases and Ni is the minor phase as was identified by X-ray diffraction analysis of Cr3C2–25NiCr coated T22 boiler tube steel specimen. The identification of small peaks of Fe and Si in XRD spectra might be due to the diffusion of these elements from substrate alloy to the coating matrix due to porosity in the matrix. The XRD spectra of 5 wt.% and 10 wt.% YSZ reinforced Cr3C2-25NiCr nanocomposite coated samples revealed major phases of Cr and Ni, along with YSZ in the coating matrix. The increase in the formation of noncrystalline amorphous phases occurs because of very fast cooling during the spraying process. Stewart *et al*. [42] reported that the presence of different phases and their proportion mostly depend on the process conditions at the time of the depositing of the coating powder on the base material.

FE-SEM with EDS analysis of conventional Cr3C2-25NiCr, 5 and 10 wt.% YSZ reinforced Cr3C2-25NiCr nanocomposite coatings on T22 boiler steel showed that coatings obtained are dense, uniform and a proper coalescence of YSZ with Cr3C2-25NiCr have been taken place and YSZ particles have been distributed uniformly within the coating matrix. Energy dispersive spectroscopy examination of all coatings revealed that the elemental composition of the various coatings was found to be comparable to that of the feedstock powder. EDS analysis of Cr3C2-25NiCr coating revealed the presence of Fe and Si in the composition, which may be due to the diffusion of Fe and Si from the substrate to the coating matrix due to porosity in conventional coating. Diffusion of base elements through pores/voids in the coating matrix has also been reported by various authors [34-37]. The cross-sectional morphology of all coatings indicated dense and uniform misconstrue. All the coatings had a uniform and intact misconstrue. Nano YSZ coatings indicated that YSZ particles had uniformly mixed in the base matrix throughout the matrix. Reinforcement of nano YSZ particles

in Cr3C2-25NiCr coating had filled the gaps, reducing porosity which prevented the diffusion of base elements to the coating matrix, thereby increasing the microhardness of the coatings.

The present study revealed that adding YSZ nanoparticles to conventional coatings improved bonding at the substrate-coating interface, filled voids/pores in the coating matrix, enhanced microhardness, and resulted in dense and uniform coatings on boiler steel samples.

Conclusions

The following conclusions are made from this experimental work:

- The thickness of HVOF sprayed Cr3C2-25NiCr, 5 wt.% and 10 wt.% YSZ reinforced Cr3C2-25NiCr nanocomposite coatings was found to be in the range of 250-260 µm.
- With the increase in YSZ concentration in nanocomposite coating, the porosity value decreases. The 10 wt.% YSZ-(Cr3C2-25NiCr) coating was discovered to have the lowest porosity value of 1.25%. A decrease in porosity resulted in an improvement in surface roughness values.
- The highest microhardness was found for 10 wt.% YSZ reinforced nanocomposite coating and was in the range of 1088-1068 hv. This might be due to the filling of pores/voids in the coating matrix by nano YSZ particles.
- XRD spectra of all nanocomposite coatings indicated the formation of non-crystalline amorphous phases due to very fast cooling during the spraying process.
- SEM/EDS analysis of Cr3C2-25NiCr coating indicated the presence of Fe and Si, which might be due to the diffusion of these elements through pores in the coating matrix. SEM/EDS analysis of YSZ reinforced nanocomposite coatings indicated a uniform and dense coating surface and there was no diffusion of base elements because of the filling up of voids/pores by nanoparticles.

Acknowledgment: *This research received no specific grant from any funding agency in the public, commercial, or not-for-profit sectors. The authors also declare that they have no conflict of interest.*

References

[1] S. Srikanth, B. Ravikumar, S. K. Das, K. Gopalakrishna, K. Nandakumar, P. Vijayan, *Engineering Failure Analysis* **10** (2003) 59-66. https://doi.org/10.1016/S1350-6307(02)00030-4

[2] S. Singh, K. Goyal, D. Bhandari, B. Krishan, *Journal of Bio-and Tribo-Corrosion* **7** (2021) 100. https://doi.org/10.1007/s40735-021-00536-1

[3] S. Kamal, K. Sharma, P. S. Rao, O. Mamat, in: *Engineering Applications of Nanotechnology,* V. Korada, B. Hisham, N. Hamid (eds.), Springer, Cham, 2017, 235-268. https://doi.org/10.1007/978-3-319-29761-3_10

[4] G. Di Girolamo, A. Brentari, E. Serra, *AIMS Materials Science* **3** (2016) 404-424. https://doi.org/10.3934/matersci.2016.2.404

[5] T. Sidhu, S. Prakash, R. Agrawal, *Journal of Materials Engineering and Performance* **15** (2006) 122-129. https://doi.org/10.1361/105994906X83402

[6] P. Puri, K. Goyal, R. Goyal, B. Krishan, *Advanced Engineering Forum* **41** (2021) 43-54. https://doi.org/10.4028/www.scientific.net/AEF.41.43

[7] R. Sivakumar, S. V. Joshi, *Transactions of the Indian Ceramic Society* **50(1)** (1991) 1-14. https://doi.org/10.1080/0371750X.1991.10804475

[8] R. Kumar, D. Bhandari, K. Goyal, *Journal of Electrochemical Science and Engineering*, **12(4)** (2022) 639-649. http://dx.doi.org/10.5599/jese.1190

[9] R.Kumar, D. Bhandari, K.Goyal, *Materials Performance and Characterization* **11(1)** (2022) http://dx.doi.org/10.1520/MPC20210080
[10] A. Röttger, S. Weber, W. Theisen, B. Rajasekeran, R. Vassen, *Materials Science and Technology* **27(6)** (2011) 973-982. https://doi.org/10.1179/1743284710Y.0000000002
[11] B. Bhushan, B. K. Gupta, *Handbook of Tribology: Materials, coatings, and surface treatments*, New York: McGraw-Hill, 1991. ISBN: 0070052492 9780070052499
[12] K. Goyal, *Tribology-Materials, Surfaces & Interfaces* **12(2)** (2018) 97-106. https://doi.org/10.1080/17515831.2018.1452369
[13] K. Szymański, A. Hernas, G. Moskal, H. Myalska, *Surface and Coatings Technology* **268** (2015) 153-164. https://doi.org/10.1016/j.surfcoat.2014.10.046
[14] K. Goyal, H. Singh, R. Bhatia. *World Journal of Engineering* **15(4)** (2018) 429-439. https://doi.org/10.1108/WJE-10-2017-0315
[15] M. Oksa, S. Tuurna T. Varis, *Journal of Thermal Spray Technology* **22** (2013) 783-796. https://doi.org/10.1007/s11666-013-9928-5
[16] J. Stokes, L. Looney, *Surface and Coatings Technology* **177-178** (2004) 18-23. https://doi.org/10.1016/j.surfcoat.2003.06.003
[17] H.S. Sidhu, B. S. Sidhu, S. Prakash, *Journal of Materials Processing Technology* **171(1)** (2006) 77-82. https://doi.org/10.1016/j.jmatprotec.2005.06.058
[18] V. Pal Singh, K. Goyal, R. Goyal. *Australian Journal of Mechanical Engineering* **17(2)** (2019) 127-132. https://doi.org/10.1080/14484846.2017.1364834
[19] S. S. Chatha, H. S. Sidhu B. S. Sidhu, *Advanced Materials Research* **1137** (2016) 88-100. https://doi.org/10.4028/www.scientific.net/AMR.1137.88
[20] M. Ksiazek, L. Boron, M. Radecka, M. Richert, A. Tchorz, *Journal of Materials Engineering and Performance* **25** (2016) 3185-3193. https://doi.org/10.1007/s11665-016-2226-x
[21] G. Kong, D. Zhang, P. D. Brown, D. G. McCartney, S. J. Harris, *Materials Science and Technology* **19(8)** (2003) 1003-1011. https://doi.org/10.1179/026708303225004684
[22] K. Goyal, H. Singh, R. Bhatia. *International Journal of Minerals, Metallurgy and Materials* **26** (2019) 337-344. https://doi.org/10.1007/s12613-019-1742-8
[23] R. Kumar, D. Bhandari, K. Goyal, *Advancement in Materials, Manufacturing and Energy Engineering,* Vol. I, *Lecture notes in Mechanical Engineering*, P. Verma, O. D. Samuel, T. N. Verma, G. Dwivedi (eds.), Springer, Singapore, 2022, pp. 277-287. https://doi.org/10.1007/978-981-16-5371-1_24
[24] J. G. Thakare, C. Pandey, M. M. Mahapatra, R. S. Mulik, *Metals and Materials International* **27** (2021) 1947-1968. https://doi.org/10.1007/s12540-020-00705-w
[25] A. V. Radhamani, H. C. Lau, S. Ramakrishna, *Journal of Composite Materials* **54(5)** (2020) 681-701. https://doi.org/10.1177%2F0021998319857807
[26] F. Ghadami, A. Zakeri, A. Sabour Rouh Aghdam, R. Tahmasebi, *Surface and Coatings Technology* **373** (2019) 7-16. https://doi.org/10.1016/j.surfcoat.2019.05.062
[27] X. Ji, X. Li, H. Yu, W. Zhang, H. Dong, *Diamond and Related Materials* **91** (2019) 247-254. https://doi.org/10.1016/j.diamond.2018.11.027
[28] K. Goyal, H. Singh, R. Bhatia, *Journal of the Australian Ceramic Society* **55** (2019) 315-322. https://doi.org/10.1007/s41779-018-0237-9
[29] A. A. Mohammed, Z. T. Khodair, A. A. Khadom, *Ceramics International* **46(17)** (2020) 26945-26955. https://doi.org/10.1016/j.ceramint.2020.07.172
[30] N. D. Prasanna, C. Siddaraju, G. Shetty, M. R. Ramesh, M. Reddy, *Materials Today: Proceedings* **5(1)** (2018) 3130-3136. https://doi.org/10.1016/j.matpr.2018.01.119
[31] Š. Houdková, Z. Česánek, E. Smazalová, F. Lukáč, *Journal of Thermal Spray Technology* **27** (2018) 179-195. https://doi.org/10.1007/s11666-017-0637-3

[32] B. M. Praveen, T. V. Venkatesha, Y. A. Naik, K. Prashantha, *Surface and Coatings Technology* **201(12)** (2007) 5836-5842. https://doi.org/10.1016/j.surfcoat.2006.10.034
[33] E. E. Anand, S. Natarajan, *Journal of Materials Engineering and Performance* **24** (2015) 128-135. https://doi.org/10.1007/s11665-014-1306-z
[34] K Goyal, R. Goyal, *Surface Engineering* **36(11)** (2020) 1200-1209. https://doi.org/10.1080/02670844.2019.1662645
[35] K. Goyal, H. Singh, R Bhatia. *International Journal of Minerals, Metallurgy and Materials* **26** (2019) 337-344. https://dx.doi.org/10.1007/s12613-019-1742-8
[36] S. S. Chatha, H. S. Sidhu, B. S. Sidhu, *Journal of Minerals and Materials Characterization and Engineering* **11(6)** (2012) 569-586. http://dx.doi.org/10.4236/jmmce.2012.116041
[37] K. Goyal, H. Singh, R Bhatia, *Anti-Corrosion Methods and Materials* **65(6)** (2018) 646-657. https://doi.org/10.1108/ACMM-06-2018-1954
[38] A. K. Keshri, V. Singh, J. Huang, S. Seal, W. Choi, A. Agarwal, *Surface and Coatings Technology*, **204(11)** (2010) 1847-1855. https://doi.org/10.1016/j.surfcoat.2009.11.032
[39] W. Guo, H.-Y. Tam*, The International Journal of Advanced Manufacturing Technology* **72(1-4)** (2014) 269-275. https://doi.org/10.1007/s00170-014-5661-6
[40] K Goyal, R. Goyal, *Surface Engineering* **36(11)** (2020) 1200-1209. https://doi.org/10.1080/02670844.2019.1662645
[41] L. Tian, Z. Feng, W. Xiong, *Coatings* **8(3)** (2018) 112. https://doi.org/10.3390/coatings8030112
[42] D. A. Stewart, P. H. Shipway, D. G. McCartney, *Wear* **225–229(2)** (1999): 789–798. https://doi.org/10.1016/S0043-1648 (99)00032-0